

THE FATIGUE LIMIT OF STEEL WIRES AS DETERMINED BY THE FATIGUE THRESHOLD AND THE SURFACE CHARACTERISTICS

I. Verpoest*, A. Deruyttere*, E. Aernoudt*, M. Neyrinck**

A new approach to the fatigue limit of steel wires is presented, which allows a quantitative assessment of the specific influence of the surface characteristics and of the bulk properties. The fatigue limit and the fatigue threshold were measured on five pearlitic steel wires which had been cold drawn to different strains and therefore to different tensile strengths. These measured values allow a prediction of the depth of the surface defects at which fatigue cracks originate. The validity of this approach is confirmed when the predicted and the observed fatigue crack origins are compared.

INTRODUCTION

Steel wires are to a great extent used in applications where vibrations or repeated shocks are the main type of mechanical loading (i.a. in springs, cables, steel reinforcements in tires and hoses, ...). Because these applications require a very high number of cycles to failure (typically 10^7 - 10^{10} cycles), the fatigue limit becomes one of the most important mechanical characteristics of high strength steel wires.

Already fifty years ago, Pomp (1) and Gill (2) carried out an extensive research on the fatigue behaviour of cold drawn, pearlitic steel wire. They proved that the ratio of fatigue limit to tensile strength decreases with increasing tensile strength (or wire drawing strain) (fig. 1). The importance of the surface condition was illustrated by the findings that decarburisation has a negative influence on fatigue strength, whereas polishing has a positive one.

Since then, enhanced production techniques improved the overall steel wire quality, but recent work, by a.o. Kloos (3) and Becker (4) simply confirmed the early conclusions of Pomp and Gill, by offering some additional evidence. However, no model seems to have been published which would explain in a coherent way the specific influence of the factors mentioned above.

A NEW APPROACH

On the one hand, a careful examination of the fatigue fracture mechanisms led us to a redefinition of the fatigue limit: *the fatigue limit is the maximum stress amplitude at which cracks, that are present before or created during the fatigue test, do not grow up to final fracture.*

On the other hand, fracture mechanics provides a useful tool to describe fatigue crack growth. In that new paradigm, *the limit between growth and non-growth of cracks is defined by the fatigue threshold*, (the stress intensi-

* Departement Metaalkunde, Katholieke Universiteit Leuven, Belgium.

** Speurwerk & Ontwikkeling, N.V. Bekaert, 8550 Zwevegem, Belgium.

ty factor range at which crack growth rates become infinitely small).

If the hypothesis is added that fatigue cracks in pearlitic steel wires are originating at surface defects, and that these defects can be treated like cracks, using the fracture mechanics approach, a simple link between the previous definitions leads to a new model for the fatigue behaviour of steel wires : "the fatigue limit σ_e of steel wires is determined by the fatigue threshold ΔK_{th} and the surface defects, which behave like cracks with dept a, according to the formula :

$$\sigma_e = \frac{\Delta K_{th}}{2 \alpha \sqrt{\pi a}} \quad [1]$$

(which is the definition formula for the stress intensity factor, but written in an unusual form).

To check the validity of this model, two parameters viz., the fatigue threshold ΔK_{th} and the fatigue limit σ_e , were measured, so that the defect depth could be predicted using formula [1]. Then, the defects from where fatigue cracks originated were measured. The agreement between the measured and the predicted defect depths is indicative for the validity of the model.

MATERIALS

This procedure was applied to five cold drawn, pearlitic steel wires of the same diameter (\emptyset 2 mm). To obtain five different tensile strengths, only the cold drawing strain and therefore the diameter at the last patenting treatment was varied. All other parameters were kept constant, the steel composition (0.66 % C, 0.72 % Mn) as well as the wire drawing processing. Mechanical stress relieving was applied after drawing. Table 1 shows the mechanical properties of these wires : with increasing drawing strain ϵ or reduction η , the yield stress σ_y and the tensile strength σ_u increase, but the reduction of area Z decreases. Surface condition is characterized by the surface roughness R_a and the maximum depth of surface defects a_{LM} , observed on longitudinal sections by means of optical microscope (fig. 2).

TABLE 1 - Mechanical Properties and Surface Condition of the Five Pearlitic Steel Wires.

code name	η (%)	ϵ (-)	σ_y (MPa)	σ_u (MPa)	Z (%)	$R_{a,max}$ (μm)	a_{LM} (μm)
2-1.3	27.6	0.32	1111	1321	58	-	-
2-1.5	61.0	0.94	1207	1469	63	1.10	10
2-1.8	85.5	1.93	1578	1855	57.9	0.92	6 + 8
2-2.1	90.5	2.35	1902	2099	51	0.84	4 + 5
2-2.2	91.9	2.51	1952	2218	49.5	-	-

EXPERIMENTAL PROCEDURE AND RESULTS

Fatigue Limit

The fatigue limit was measured in a statistical way, using a procedure proposed by Dengel (5). Tests were carried out on a servohydraulic fatigue

testing apparatus at a frequency of 30 Hz. A constant mean tensile stress of 600 MPa was applied, and afterwards the fatigue limits at $R = 0$ and $R = -1$ were calculated using a Goodman-Smith diagram. Figure 1 shows how the ratio of fatigue limit to tensile strength decreases with increasing tensile strength.

Fatigue Threshold

To measure the fatigue threshold, a technique had to be found which would allow the detection and continuous measurement of small cracks in fine steel wires during fatigue tests.

A high frequency (10 kHz), low current density (1A) AC-potential drop method has been developed for that purpose. A very stable and sensitive lock-in amplifier and a specially designed differential detector permits the detection of cracks as small as 40 μm , and the measurement of crack growth increments as low as 2.7 μm (Verpoest, 6,7).

Once a crack grows to about 200 μm length, a load shedding technique (at $R = 0$) is applied to obtain crack growth rates as low as 10^{-8} mm/cycle at final crack lengths of 400 to 800 μm . A double logarithmic, linear regression is carried out on all data points with $\frac{da}{dN} < 10^{-6}$ mm/c, and the fatigue threshold is defined at 10^{-7} mm/c. Figures 3 and 4 show some typical results for lower strength ($\sigma_u = 1300$ MPa) and high strength ($\sigma_u = 2200$ MPa) steel wires.

It was found that the fatigue threshold decreases when the drawing strain, and therefore the tensile strength, increases (fig. 5). However, for high strength steel wires ($\sigma_u > 2000$ MPa) the fatigue threshold remains constant at about 3.5 MPa/m. Comparison with literature data on pearlitic steels could hardly be done, because all but one data points are in the tensile strength range from 500 to 1000 MPa (Verpoest, 8). However, fatigue thresholds for martensitic steels follow the same trend (Ritchie, 9; Vosikovsky, 10; Lindley, 11; Gu, 12).

The validity of the application of linear-elastic fracture mechanics and of the load shedding procedure could be proved for four of the five steel wires. Only for the one with the lowest tensile strength, the crack growth increments at each load level were too small compared to the plastic zone size. This resulted in a retardation of the crack growth, and so in an overestimation of the fatigue threshold.

APPLICATION OF THE NEW MODEL

Prediction of the Defect Size

Introducing ΔK_{th} and σ_e in formula [1], the depth of defects at which fatigue cracks originate was calculated, modelling the defects as semi-circular surface cracks with $\alpha = 0.67$.

Figure 2 (upper line) shows that this calculated defect depth decreases with increasing tensile strength. The surface roughness follows the same trend (fig. 2, lower line), although its absolute value is far too small. Optical measurements on longitudinal sections revealed some larger defects than the surface roughness suggests (fig. 2, medium line). However, the probability that these longitudinal sections are crossing the deepest defects is rather small.

Characterisation of Crack Origins

The only way to check the validity of the former prediction was to measure the real fatigue crack origins. An extensive scanning electron microscope study on about 150 wires, broken after stress cycling just above the fatigue limit, revealed various types of defects at which fatigue cracks originated. It was proposed to model each defect by a semi-elliptical surface crack, with depth a and width $2c$ (Verpoest, 8). From data by Newman (13), a relation could be derived between the geometrical factor α and the depth-to-width ratio $\frac{a}{c}$:

$$\alpha = - 0.139 \left(\frac{a}{c}\right) - 0.314 \frac{a}{c} + 1.123 \quad [2]$$

If we introduce formula [2] in [1] and apply some more statistics, we can construct the 95 % probability bands for the predicted defect depths as a function of the defect geometry $\frac{a}{c}$ (fig. 6-7). In the same figures, each crack origin, characterised in the SEM-study, is represented by a dot.

Validity of the Model

Figure 7 is representative for the higher strength steel wires ($\sigma_u > 1800$ MPa) : the agreement between the measured and the predicted defect depth and geometry is very good. This means that for these wires the model is applicable; from a theoretical point of view it was proved additionally (Verpoest, 8) that these three-dimensional defects indeed act like two-dimensional cracks as soon as a very small crack ($< 1 \mu\text{m}$ or some interlamellar distances) is present or created in the bottom of the defect. Consequently, LEFM can be applied straightforwardly.

On the contrary, this is not the case for the lower strength steel wire ($\sigma_u = 1500$ MPa), because a large plastic zone is formed around the initial defect. As a consequence, the predicted and the measured crack origins do not coincide (fig. 6) and the model is not applicable, unless an elasto-plastic analysis can be made.

CONCLUSIONS

A new model has been developed, which allows a qualitative and quantitative explanation of the specific influence of surface characteristics and bulk properties on the fatigue limit of cold drawn, pearlitic steel wires. The fatigue threshold is the key bulk property, whereas in this study the size and shape of individual surface defects (and not the overall surface roughness) are the most important surface characteristics. It is the opinion of the authors that the influence of decarburization, polishing and other parameters can be explained in an analogous way by this model.

REFERENCES

1. Pomp, A. and Duckwitz, C.A., 1931, Mitteilungen aus dem Kaiser Wilhelm Institut, XIII, 79.
2. Gill, E.T. and Goodacre, R., 1934, J. Iron & Steel Inst., 130, 293.
3. Kloos, K.H. and Pepler, P., 1976, Wire, 26, 1.
4. Becker, K., 1978, Wire Ind., 531.
5. Dengel, D., 1978, in "Verhalten von Stahl bei Schwingender Beanspruchung", Verlag Stahleisen, Düsseldorf, 23.
6. Verpoest, I. et al., 1981, Fatigue of Eng. Mat. & Struct., 3, 203.
7. Verpoest, I. et al., 1982, in "Crack Length Measurement II", EMAS, Warley, (U.K.).

8. Verpoest, I., 1982, Ph.D.-thesis, Cath. University, Leuven, Belgium.
9. Ritchie, R.O., 1977, *Metals Science*, 11, 368.
10. Vosikovskiy, O., 1979, *Eng. Fract. Mech.*, 11, 595.
11. Lindley, T.C. and Richards, C.E., 1982 in "Fatigue Thresholds", EMAS, Warley (U.K.).
12. Gu, H. and Knott, J.F., 1981, in "Fatigue Thresholds", EMAS, Warley (U.K.).
13. Newman, J.C., 1979, in "Part-Through Crack Fatigue Life Prediction", ASTM-STP 687, 16.

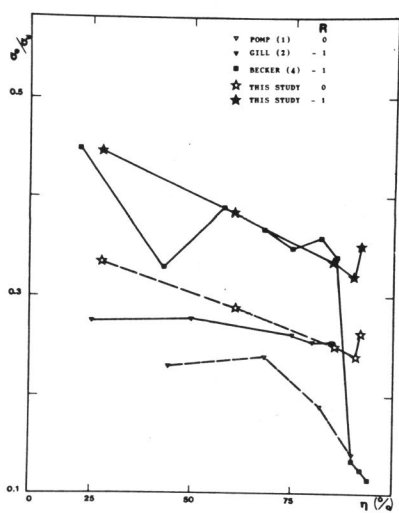


Fig. 1. Fatigue limit to tensile strength ratio for different wire drawing reductions.

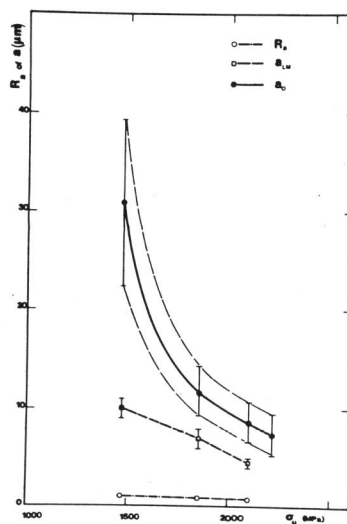


Fig. 2. Surface roughness parameters as a function of tensile strength.

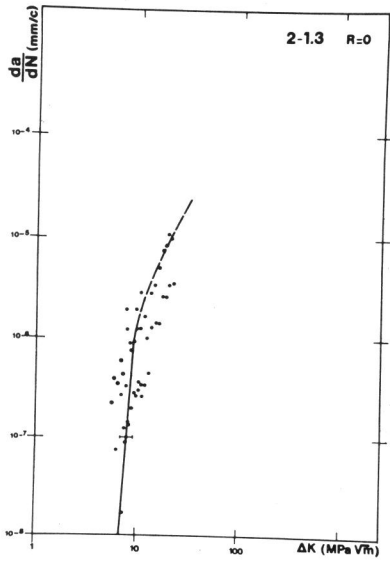


Fig. 3. Fatigue crack growth rate versus stress intensity factor range for wire 2-1.3 at R = 0.

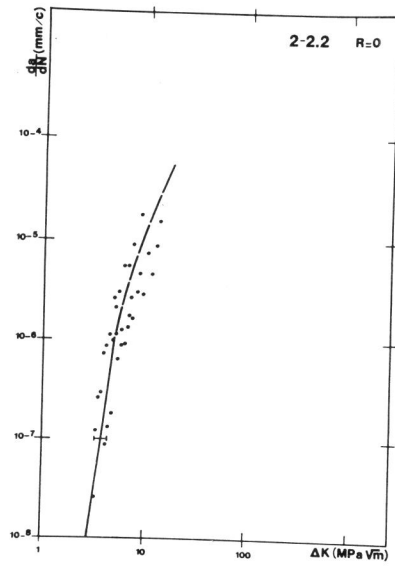


Fig. 4. Idem fig. 3 for wire 2-2.2 at R = 0.

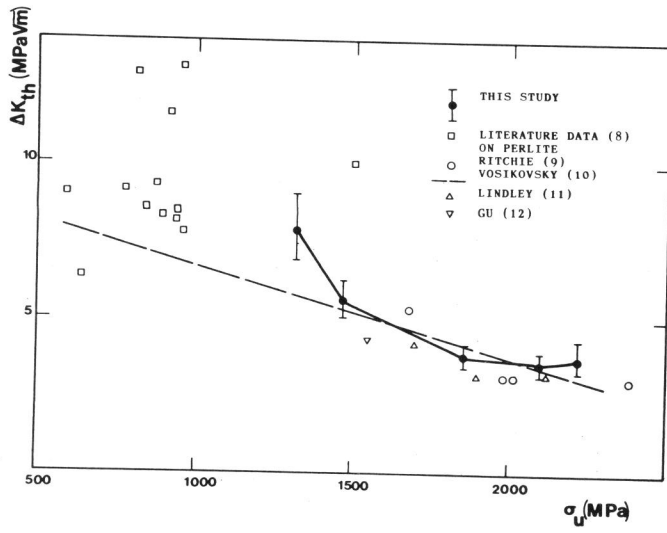


Fig. 5. Fatigue threshold at R = 0 as a function of tensile strength.

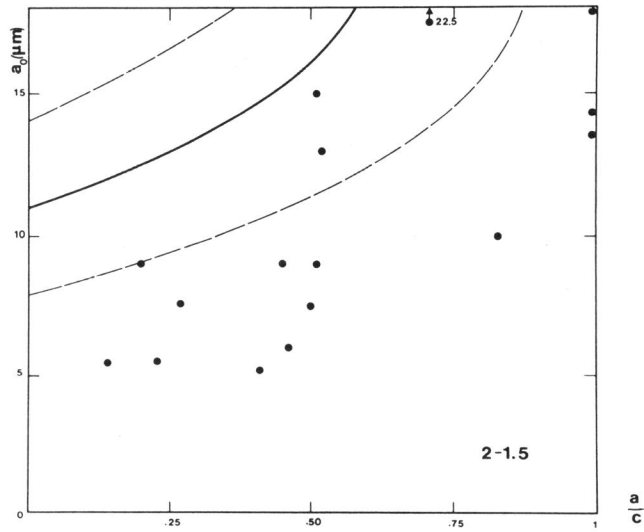


Fig. 6. Comparison between observed (●) and predicted (full line with 95 % confidence limits) defect depths for wire 2-1.5 at $R = 0$.

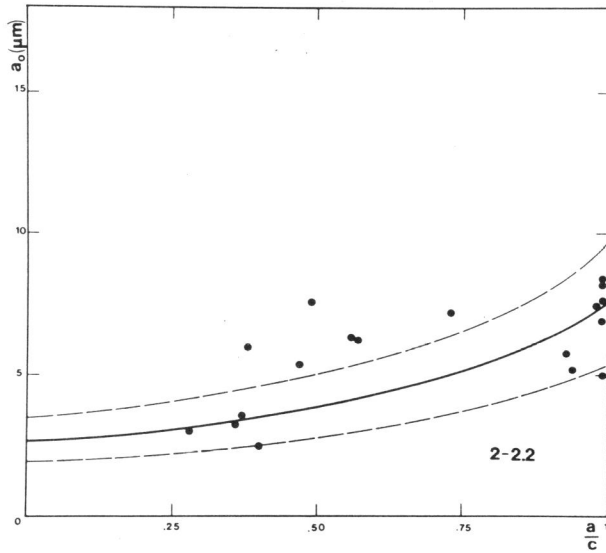


Fig. 7. Idem fig. 6, for wire 2-2.2 at $R = 0$.